Composites of High-Temperature Thermomechanical Pulps and Polylactic Acid

Iina Solala,[a,*] Antti Koistinen,[a] Sanna Siljander,[b] Jyrki Vuorinen,[b] and Tapani Vuorinen [a]

High-temperature thermomechanical pulps (HT-TMP, defibrated at 150 to 170 °C) were compared to a reference TMP (defibrated at 130 °C) as a reinforcement for polylactic acid (PLA). Composites were prepared by melt compounding, followed by injection molding, gradually increasing the used fiber content from 0 to 20 wt.%. The injection-molded specimens were characterized by tensile and impact strength tests, scanning electron microscopy, water absorption tests, and differential scanning calorimetry. The TMP fiber damage was also characterized before and after melt compounding by optical analysis. At 20% fiber content, the Young's modulus increased significantly, while the tensile strength remained unchanged and the impact strength decreased slightly. All fibers suffered damage during melt compounding, but the tensile strength remained about the same as in pure PLA. All types of TMP were able to increase the PLA rate of crystallization. The HT-TMP fibers were dispersed more evenly in PLA than the 130 °C TMP. The 170 °C TMP produced composites of lower water absorption than the other two TMP types, probably because of its lower hemicellulose content and its higher surface coverage by lignin.

Keywords: Polylactic acid; High-temperature thermomechanical pulp; Hydrophobic fibers; Wood fiber composites; Thermal properties; Mechanical properties

*Contact information: a: Department of Forest Products Technology, School of Chemical Technology, Aalto University, Espoo, Finland; b: Department of Materials Science, Tampere University of Technology, Tampere, Finland; *Corresponding author. Current contact details: iina@chalmers.se; Department of Chemistry and Chemical Engineering, Chalmers University of Technology, Kemigården 4, 41258 Gothenburg, Sweden*

INTRODUCTION

Minimizing environmental impact is one of the main driving forces in the development of new materials. How 'green' a given material can be regarded is determined by a number of factors, such as renewability, recyclability, biodegradability, and energy consumption during manufacturing. Common commercial plastics are generally derived from petroleum sources, resulting in CO_2 emissions and accumulation of plastic waste. A significant body of research has been devoted to the development of biodegradable plastics, most of which are derived from biomass. Out of the commercially available biodegradable plastics, polylactic acid (PLA) is the most promising. It is a thermoplastic biodegradable aliphatic polyester, commonly derived from corn or potato. Depending on its isomer composition, it can be highly crystalline (pure L-lactic acid) or completely amorphous (racemic mixture of L- and D-lactic acids), and the thermal and optical properties vary greatly according to crystallinity (Drumright *et al.* 2000; Nampoothiri *et al.* 2010).

The relatively high cost of PLA still limits its usability as a commodity plastic, although its cost has decreased in recent years. One possible solution to this would be to introduce low-cost fillers or reinforcing agents to PLA. In the interest of maintaining the

biodegradability of the PLA, natural fibers, such as wood-based fibers, are a logical choice. Wood consists of cellulose, lignin, hemicelluloses, and extractives, and the relative amounts of these components vary according to wood species, tissue type, and so on. Furthermore, different cell wall layers have chemical compositions (*e.g.*, the middle lamella layer that holds fibers together is rich in lignin, whereas the secondary wall contains more cellulose and hemicelluloses). Largely because of the cellulose and hemicellulose components, wood-derived fibers tend to be hydrophilic, which can cause compatibility problems with hydrophobic commercial plastics.

One strategy to overcome the compatibility problem would be to prepare wood-based fibers of increased hydrophobicity, using a modified thermomechanical pulping (TMP) process, in which high temperatures (HT, 150 to 170 °C, instead of the more common 120 to 130 °C) are used. This way, a high yield of the initial wood material can be achieved, while avoiding the common problem of thermomechanical pulping – its high specific energy consumption. The weak interfiber bonding that is characteristic of these HT-TMPs (Roffael *et al.* 2001; Widsten *et al.* 2001, 2004; Gustafsson *et al.* 2003) is considered a drawback in papermaking, where a strong fiber network is desired, but it may even be an advantage in composite applications, where uneven fiber dispersion in the matrix is a common obstacle. It has also been proposed that the abundance of lignin in TMPs enhances their adhesion to hydrophobic matrices (Peltola *et al.* 2014; Solala *et al.* 2014).

Current industrial use of HT-TMP is restricted to the manufacturing of medium density fiberboard (MDF). Typically, urea-formaldehyde resins are used as the adhesives in MDF, but other, more environmentally benign alternatives have been suggested (Widsten *et al.* 2004; Xing *et al.* 2005; Widsten and Kandelbauer 2008; Valenzuela *et al.* 2012; Wu *et al.* 2015). Given that industrial scale facilities for HT-TMP manufacturing, *i.e.*, traditional TMP mills, already exist, using HT-TMP in biocomposites should be relatively straightforward. As long as the mills have a well optimized heat recovery system, the production of HT-TMP is expected to consume significantly less energy than conventional TMP manufacturing (Solala *et al.* 2014).

For these reasons, cheap HT-TMP seems like a promising candidate for reducing the cost of PLA-based composites. In this paper, we propose a new use for the HT-TMP, namely, its application in PLA-based biocomposites. To the best of our knowledge, this is the first study to cover the thermal, mechanical, and water absorption properties of melt-compounded injection molded HT-TMP/PLA composites. Previous studies, such as those of Peltola *et al.* (2011, 2014), have described the use of conventional TMP and other wood-derived fibers.

EXPERIMENTAL

Materials and Methods

Preparation of TMP fibers

The TMP fibers (dimensions given in Table 1) were prepared in a wing refiner (Defibrator Ab, Stockholm, Sweden) as described by Solala *et al.* (2014) by filling the defibrator with 100 to 120 g of spruce (*Picea abies* L.) chips at approximately 35% consistency, steaming the chamber evenly with 130, 150 or 170 °C steam, and refining for 2 min. Spruce is conventionally used in industrial TMP manufacturing, which is why it was selected for this study as well.

The properties of these fibers have been described elsewhere (Solala *et al.* 2014), but the key differences between the reference (130 °C) TMP and the HT-TMP (150 to 170 °C) are higher surface coverage by lignin, weaker fiber-fiber bonding, and a loss of hemicelluloses at high defibration temperatures, especially for the 170 °C TMP. The TMP prepared at 170 °C also developed a darker color than the other two TMP types. According to previous studies on thermal treatment of softwood in dry and moist conditions (Sivonen *et al.* 2002; Pétrissans *et al.* 2003; Yin *et al.* 2011), the equilibrium moisture content is expected to be lower for the HT-TMPs. This can be at least partly explained by the degradation of hemicelluloses at elevated temperatures. Thermal treatments have also been shown to decrease wood toughness, and similar changes presumably occur at the fiber level as well.

The resulting TMPs were screened with a 0.2-mm slot plate until no separate fibers remained in the reject fraction. The accepted fraction was centrifuged to remove excess water and homogenized for 5 min before storing at -20 °C. Before using, the TMPs were first pre-dried at room temperature until the dry matter content was approximately 90% and later fully dried (105 °C, 12 h) before melt-compounding. The PLA was pre-dried at 70 °C for 12 h.

Preparation of composites

The composites were prepared by melt-compounding fully dry PLA (Ingeo 3052D, purchased from NatureWorks LLC, USA) and fibers at 185 °C in a 5-mL DSM Xplore co-rotating twin-screw microextruder (Xplore Instruments, Netherlands). The fibers were not pre-treated in any other way than drying, and they were manually added to the molten PLA using a funnel. First trials were carried out at 150 rpm; based on the work of Gamon *et al.* (2013), we also wanted to determine whether or not fiber damage could be limited by using a higher mixing rate, namely, 225 rpm. The barrel temperature was 190 °C at all times, and the estimated time of residence in the microextruder was 5 min for the TMP fibers. The used weight percentages of TMP in the composite were gradually increased from 0 to 20% to see how high a fiber fraction it was possible to use without damaging the microextruder. A force sensor was used to evaluate how much fiber could be incorporated; in practice, 3000 N was selected as the upper limit. In other words, the achievable fiber content in the DSM microextruder was lower than the more common industrially used fiber content of 20 to 40%. Another limitation of the used microextruder is that it may have caused more severe fiber damage than is typical for larger industrial extruders.

Dog bone-shaped specimens for tensile strength (EN ISO 527-2-1BA) and rectangular standard specimens for unnotched Charpy impact strength (EN ISO 179-1/1e) measurements were then injection molded with the DSM, operating at an injection pressure of 6 bar, using a nozzle temperature of 190 °C and a mold temperature of 50 °C.

Characterization of fiber morphology

It is well known that extrusion causes damage to natural fibers (Le Baillif and Oksman 2009; Peltola *et al.* 2014). Thus, optical analysis was carried out with a commercial Kajaani FiberLab (Metso Automation, Finland) device, yielding information on the fiber length and width distributions before and after melt compounding (Table 1, Fig. 1). Initial air-dry TMP was dispersed in water and analyzed according to the TAPPI T271 om-98 standard with the following modifications: tap water was used to dilute the sample to a consistency of approximately 0.06 g/L. Another modification was that with the

high-temperature samples, more clogging took place, so the number of analyzed fibers had to be decreased by picking up the largest, splinter-like particles.

To characterize the TMP fiber properties after the extrusion, the PLA was removed by 5-h Soxhlet extraction with chloroform (analysis grade, Merck) until no PLA could be seen on the fiber surfaces. It is possible that residual PLA or the chloroform treatment itself have altered the swelling properties of the fibers, meaning that the values for thickness should be interpreted with caution. However, the fiber length values should be less susceptible to such changes and thus more reliable.

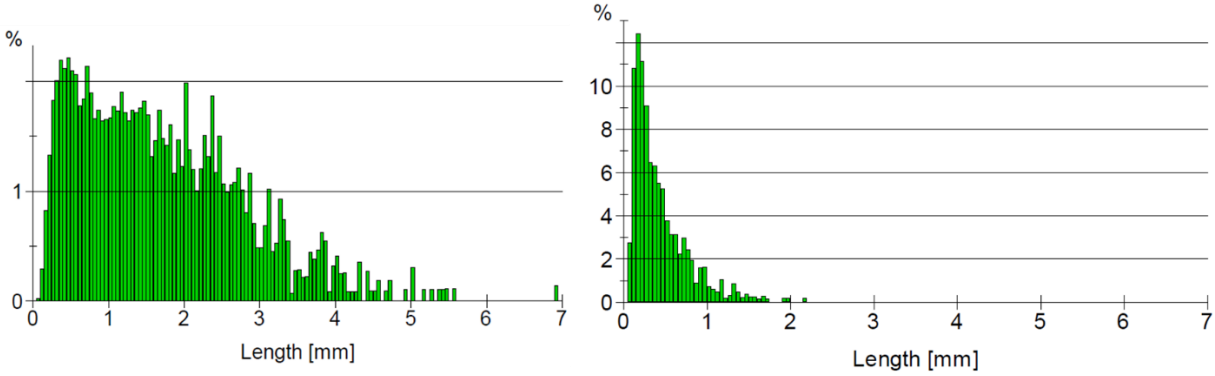

Fig. 1. An example of the fiber length distributions before (left) and after (right) melt-compounding, showcasing the extensive fiber damage that took place in 130 °C TMP

Mechanical testing and scanning electron microscopy

Prior to mechanical testing, the specimens were conditioned at 23 °C and 50% relative humidity for at least 48 h. Tensile properties were recorded according to EN ISO 527-2-1BA from dog bone-shaped specimens with dimensions of approximately 2.1-mm thickness and 5.5-mm width with an Instron 5967 Universal Tensile Tester (Instron Corp. Canton, MA, USA). The average of five samples was calculated for each sample type. Charpy impact strengths were measured according to EN ISO 179-1/1e from unnotched specimens of dimensions 80 mm * 10 mm * 4 mm with a Ceast Resil 5.5 Impact Strength Machine (CEAST S.p.a., Torino, Italy) using a 4-J pendulum. The average of ten samples was calculated for each sample type.

Scanning electron microscopy (SEM) was used to examine the fracture mechanism in the tensile specimens. For this purpose, small pieces were sawn from the vicinity of the fracture surface. The specimens were then attached to sample holders, fracture surface upward, carbon sputtered for 10 s, and imaged with a Hitachi (Japan) TM-1000 tabletop SEM using an acceleration voltage of 15 kV.

Thermal testing by differential scanning calorimetry

Differential scanning calorimetry (DSC 204 F1, Netzsch, Germany) was used to estimate the glass transition and melting temperatures (T_g and T_m, respectively), as well as the level of crystallinity of the PLA and the composites. Approximately 10 mg of sample was weighed on an aluminum pan and heated from 25 to 220 °C with a heating rate of 20 °C/min in a N_2 atmosphere (20 mL/min). Two parallel specimens were measured, with two heating cycles.

The level of crystallinity, X (%), was estimated using Eq. 1:

$$X(\%) = 100 * \frac{\Delta H_m - H_c}{\Delta H_{m,0}} \quad (1)$$

where ΔH_m is the enthalpy of melting, H_c is the enthalpy of cold crystallization, and $\Delta H_{m,0}$ is the enthalpy of melting for 100% crystalline PLA. The values in the numerator were obtained as the areas under the appropriate peaks in the DSC graphs, using the data from the second heating runs. The used value for the denominator was 93 J/g, although some sources report slightly different values (Gamon *et al.* 2013).

Water absorption

To estimate the water absorption of the composites of 20% fiber content, EN ISO 62:2008 (Method 1) was slightly modified, only by changing the specimen shape. Rectangular Charpy impact strength specimens (80 mm * 10 mm * 4 mm) were injection-molded and sawn at one end. The specimens (three parallel specimens for each sample type) were first dried at 50 °C in a vacuum oven for 24 h, cooled in a desiccator and weighed, then immersed in 23 °C ultrapure water, dried on the surface by Whatman filter paper, and weighed again after immersion times of 24, 48, 96, 168, 216, and 312 h.

RESULTS AND DISCUSSION

Dispersion in PLA and Changes in Fiber Morphology

In general, the composites were easy to prepare up to a fiber content of approximately 20 wt.%. However, there were clearly visible differences in fiber distributions in the PLA matrix (Fig. 2).

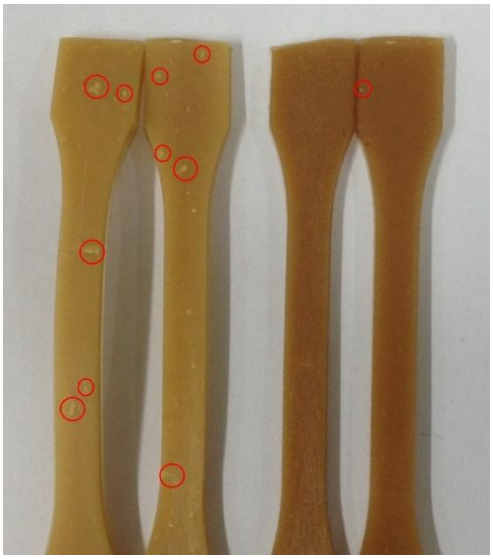

Fig. 2. Dog bone-shaped tensile specimens of 130 °C (left) and170 °C (right) TMPs had visible differences in fiber dispersion and in composite color. Selected fiber flocs have been highlighted with red circles.

The HT-TMPs produced composites with little to no visible fiber flocs, but the 130 °C TMP contained poorly dispersed fiber agglomerates. The reason for the poor dispersion of the 130 °C TMP is most likely their higher level of fibrillation and thus their

higher fiber-fiber bonding ability (Solala *et al.* 2014); furthermore, the high surface coverage by lignin (measured by X-ray photoelectron spectroscopy and confirmed with scanning and transmission electron microscopies by Solala *et al.* 2014) probably contributed to the easier dispersion of the HT-TMPs. It is also clear that the composites prepared from the 170 °C HT-TMP had a darker color than the corresponding composites made from the 130 °C TMP (Fig. 2). There was a similar difference in color also visible in the initial fibers.

Comparison of the original TMPs (Table 1) revealed initial differences in fiber length and width, as well as in curl percentage. The fiber lengths and widths were consistently higher at elevated defibration temperatures, whereas the curl values were lower, supporting the notion that HT-TMP fibers are stiffer and more intact than conventional TMP (Gustafsson *et al.* 2003; Solala *et al.* 2014). Before melt compounding, the fines content was roughly the same for all sample types, perhaps slightly lower for the 170 °C HT-TMP. The term 'fines' refers to the fiber fraction that can pass through a round hole of a diameter of approximately 76 µm (according to the TAPPI standard T261 pm-80). Generally, the specific surface area will increase as particle size increases, leading to effective interfacial bonding (Ahmed and Jones 1990). On the other hand, a decrease in fiber aspect ratio may decrease the strength properties if the fiber length is not at a sufficient level.

Table 1. Fiber Properties Before and After Melt Compounding at Various Conditions

Sample type	Length (mm)	Width (µm)	Fines (%)	Curl (%)	Kink (1/m)
Initial TMP 130	1.6 ± 0.1	26.0 ± 0.4	19 ± 3	16.1 ± 0.8	-
Initial TMP 150	2.1 ± 0.1	27.4 ± 0.4	22 ± 2	10.8 ± 0.8	414 ± 15
Initial TMP 170	2.4 ± 0.1	30.9 ± 0.6	15 ± 3	9.5 ± 0.3	232 ± 22
Ext-TMP 130 5% 150 rpm	0.45 ± 0.00	25.3 ± 0.1	32.4 ± 0.9	10.4 ± 0.1	1010 ± 15
Ext-TMP 150 5% 150 rpm	0.26 ± 0.02	26.0 ± 0.5	64.0 ± 0.7	6.3 ± 0.1	341 ± 47
Ext-TMP 170 5% 150 rpm	0.25 ± 0.01	26.4 ± 0.2	32.4 ± 0.9	6.1 ± 0.2	361 ± 1
Ext-TMP 130 20% 150 rpm	0.40 ± 0.01	26.4 ± 0.1	64.0 ± 0.7	11.4 ± 0.0	764 ± 54
Ext-TMP 150 20% 150 rpm	0.17 ± 0.01	28.8 ± 0.6	60.5 ± 0.2	5.7 ± 0.1	147 ± 13
Ext-TMP 170 20% 150 rpm	0.18 ± 0.00	30.0 ± 0.7	37.0 ± 0.1	4.0 ± 0.1	73 ± 17
Ext-TMP 130 20% 225 rpm	0.35 s± 0.01	25.7 ± 0.3	77.0 ± 0.1	8.2 ± 0.3	337 ± 20
Ext-TMP 150 20% 225 rpm	0.23 ± 0.00	33 ± 6	75 ± 1	5 ± 1	255 ± 4
Ext-TMP 170 20% 225 rpm	0.23 ± 0.01	30.1 ± 0.4	47.5 ± 0.3	4.7 ± 0.2	-

The prefix Ext- refers to extrusion. The errors are indicated as standard deviations for 2 to 4 parallel measurements, depending on how much the values deviated from one another. All values are weight-averaged values, except the curl values

The high shear and temperature of the extrusion caused a dramatic drop in fiber length, but fiber width remained practically unaffected by the process, as was expected. Fiber aspect ratios of the melt-compounded HT-TMPs (Fig. 3) were close to typical values for wood flour composites (Migneault *et al.* 2008; Hietala *et al.* 2011), whereas the aspect ratios of the 130 °C TMP were slightly higher for both mixing rates, indicating that the TMP produced at 130 °C was more resistant to the thermomechanical damage. Use of the lower fiber contents (5%) resulted in a slightly less severe fiber damage than what was observed for 20%, as expected.

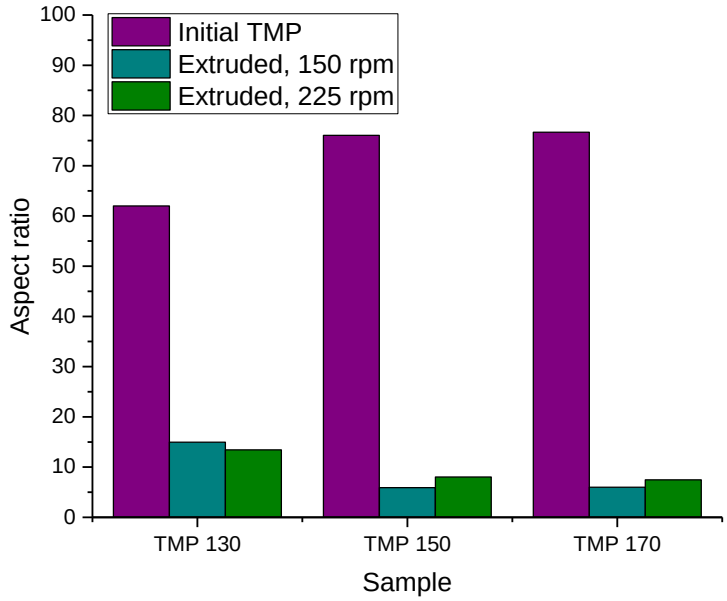

Fig. 3. Fiber aspect ratios (fiber lengths divided by fiber widths) before and after melt-compounding and injection molding at 20 wt.% TMP

Because all fibers were in their dry state during the melt compounding, they were expected to be in a hard/brittle state at the used temperature; native lignin softens only above 205 °C when dry (Salmén 1982). This leads to fiber cutting occurring more frequently than fiber fibrillation. Furthermore, analogously to the way solid wood pieces lose their toughness upon thermal degradation (Sivonen *et al.* 2002), the high defibration temperatures (150 to 170 °C) likely caused initial embrittlement of the fibers (Yin *et al.* 2011), which led to the observed difference in fines content. It is also possible that because the 130 °C TMP was not dispersed as evenly in PLA, the presence of fiber flocs protected the inner parts of the fiber agglomerates, leading to the less extensive fiber damage observed in the 130 °C TMP.

Based on the fiber length analyses after melt-compounding at 150 and 225 rpm, the attempt to limit fiber damage by increasing the mixing rate did have a small effect on fiber damage. The 130 °C TMP was damaged less at 150 rpm than at 225 rpm (Table 1) but the opposite was observed for the HT-TMPs: their fiber lengths remained at a slightly higher level after being melt-compounded at 225 rpm. Based on this, some modest improvements in fiber length may be obtained by optimizing the conditions of melt compounding, but further studies will be needed to confirm this.

Mechanical Properties and Fracture Mechanism

Mechanical properties of the 20 wt.% fiber composites extruded at 150 rpm are summarized in Table 2. The density did not change significantly upon the introduction of the TMP fibers ($\rho = 1.27 \pm 0.01$ g/mL for pure PLA and 20% TMP composites), meaning that simple comparisons of the mechanical properties should be possible. The tensile strength and elongation at break did not change in any major way after the addition of TMP; the impact strength decreased by roughly 30% from the value of pure PLA. The Young's modulus increased, especially for the HT-TMPs.

Table 2. Mechanical Properties of the Extruded PLA and Composites (20 wt.%) with the Different TMPs

Sample type	Tensile strength (MPa)	Young's modulus (GPa)	Elongation at break (%)	Impact strength (kJ/m^2)
Ext-PLA	57 ± 1	2.9 ± 0.4	3 ± 1	17.4 ± 0.7
Ext-TMP 130 20%	51 ± 5	4.5 ± 0.5	4 ± 1	12 ± 1
Ext-TMP 150 20%	59 ± 1	5.4 ± 0.7	3.8 ± 0.3	12 ± 2
Ext-TMP 170 20%	56 ± 3	5.6 ± 0.4	3 ± 1	13 ± 2

Number of parallel specimens: five for tensile strength, Young's modulus, and elongation at break; ten for impact strength. Errors as one standard deviation

Mechanical properties depend on the fiber volume fraction and length, the latter being much more important in terms of tensile properties (Fu and Lauke 1996; Fu *et al.* 2000). Composite stiffness, *i.e.*, Young's modulus, is less sensitive to changes in fiber length and mostly depends on the fiber volume fraction (Fu *et al.* 2000), as was seen in our experiments as well. Impact strength is more sensitive toward adhesion problems, resulting in typically low impact strength values of natural fiber composites (Saheb and Jog 1999; Li and Sain 2003). This is a potential topic for a follow-up study where the effect of reactive coupling agents on the mechanical properties would be tested. On the other hand, fiber-matrix adhesion is not the only parameter that influences the impact strength, and it is possible that the low elongation at break values of the TMP fibers contribute to the decrease in impact strength (Wambua *et al.* 2003).

Even at 20 wt.% fiber content, no increase in tensile strength could be seen in any of the composites (Fig. 4). However, it should be noted that large-scale extruders are commonly used for fiber contents as high as 40%, so the melt-compounding method employed in this study is not directly comparable to existing industrial processes. It is possible that an increase in tensile strength would be achieved at higher fiber contents.

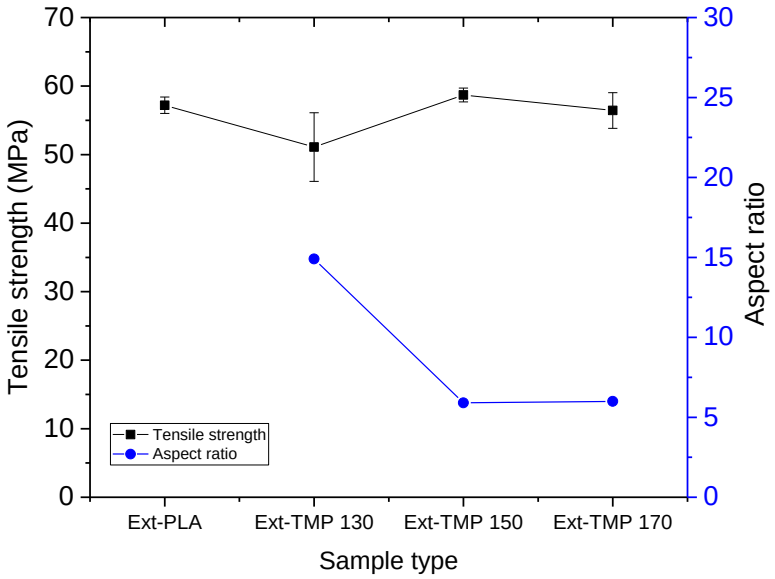

Fig. 4. Tensile strengths of PLA and its composites (20 wt.%; defibration temperatures of 130, 150, and 170 °C) after extrusion at 150 rpm (black squares). The corresponding fiber aspect ratios are shown as blue circles.

Assuming that both the fiber length and the interfacial adhesion were at a sufficient level, it is possible that a reinforcing effect would be achieved by further increasing the fiber content to 30 to 40 wt.% (Migneault *et al.* 2009; Peltola *et al.* 2014). Peltola *et al.* (2014) reported a notable increase in tensile strength (77 MPa *vs*. 61.5 MPa for neat PLA) for 30 wt.% H_2O_2-bleached TMP with an average length of 0.43 mm. According to Koljonen *et al.* (2003), peroxide bleaching has only a very limited influence on the surface lignin of TMP fibers. It is therefore likely that the 0.35 to 0.40 mm length of our 130 °C TMP was not the reason for the lack of a reinforcing effect. Surprisingly, the 130 °C TMP did not produce stronger composites than the HT-TMPs, even if it had a higher aspect ratio (Fig. 4) – on the contrary, for the composites prepared at 150 rpm, its tensile strength was slightly lower than that of the composites containing HT-TMP, indicative of a slight improvement in the fiber-matrix adhesion for the HT-TMPs.

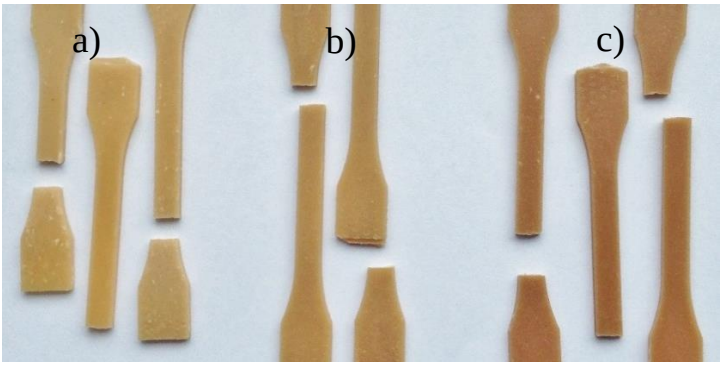

Fig. 5. The fractured tensile specimens were fractured in a brittle manner, regardless of the used TMP type. The used TMP types: a) 130 °C, b) 150 °C, and c) 170 °C; fiber content: 20 wt.%.

Visual inspection of the tensile specimens indicated that the specimens had fractured in a brittle manner (Fig. 5). As could be seen in Fig. 2 as well, the 130 °C TMP was less evenly dispersed in the matrix, containing fiber bundles that were visible also in the SEM images (Fig. 6a). The 150 °C fibers were much more evenly distributed in the PLA matrix (Fig. 6b), showing only occasional fiber pull-out from the matrix. Also, the 170 °C TMP fibers were evenly distributed, but showed more pull-out from the matrix, as well as holes surrounding the fibers (Fig. 6c). In many cases, the pulled out fiber segments had a microfibril angle parallel to the fiber axis, meaning that the S2 layer of the secondary wall was revealed. According to Solala *et al.* (2014), lignin-rich middle lamella fragments are more frequently present on the fiber surfaces of the 170 °C TMP. For this reason, it seems plausible that these lignin-coated fibers have strong enough adhesion with the PLA to favor fiber delamination, *i.e.*, cell wall fracture, over the pull-out of intact fibers, especially because the transition zone between S1 and S2 layers of softwood secondary walls has been identified as the weakest region of the cell wall (Brändström *et al.* 2003; Gustafsson *et al.* 2003). It should also be noted that thermal treatments cause degradation in glucomannan (Yin *et al.* 2011), the hemicellulose that is typically enriched at this S1/S2 boundary of conifer fibers (Donaldson and Knox 2012), implying that the 170 °C TMPs may have suffered additional weakening in the S1/S2 region because of the elevated defibration temperature. Sugar analyses by Solala *et al.* (2014) confirmed a loss of mannose in 170 °C TMPs, supporting this view. However, these suppositions still require further confirmation.

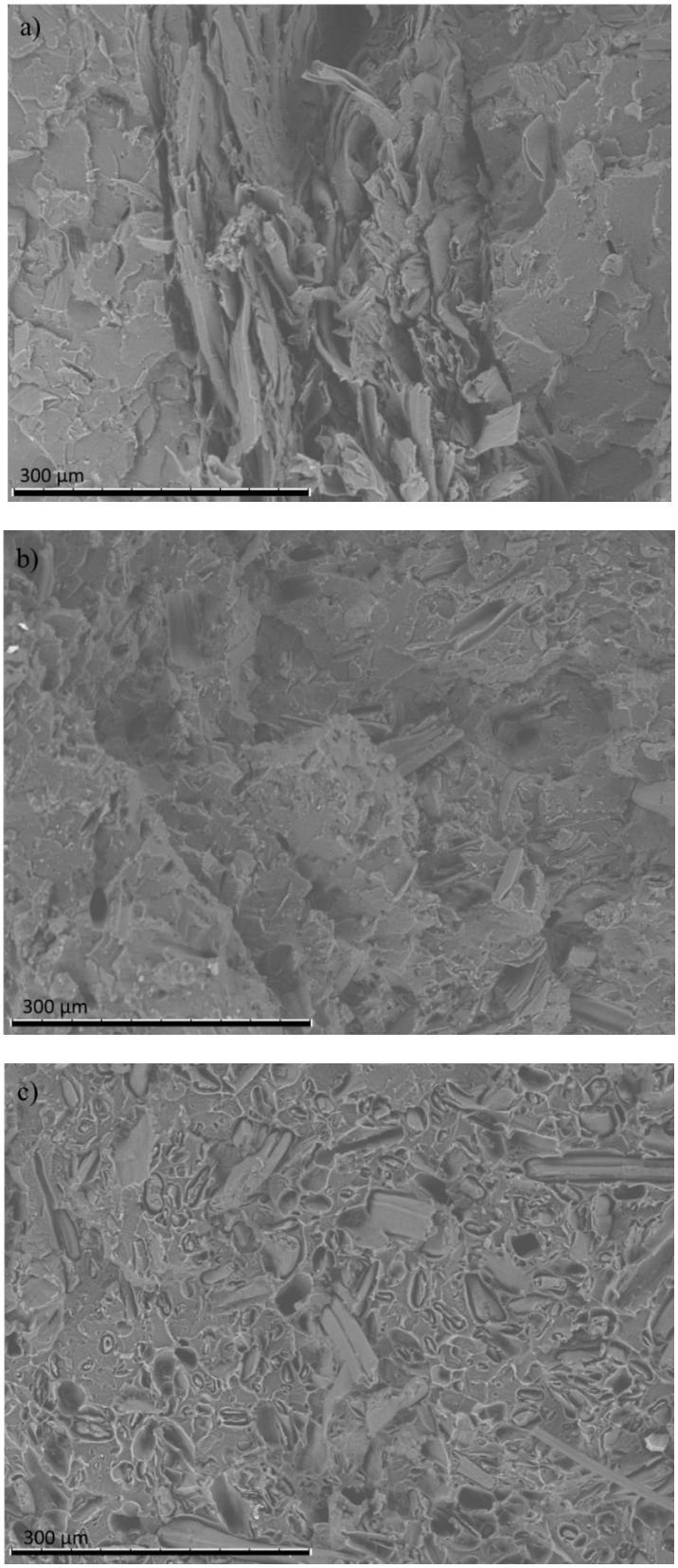

Fig. 6. SEM images of fracture surfaces of TMP/PLA (20 wt.% fiber, 150 rpm) tensile specimens. a) 130, b) 150, and c) 170 °C TMP. The scale bar shows 300 µm.

Thermal Properties

The results of the DSC measurements (Table 3) showed no major changes in transition temperatures after fiber addition. The T_g and T_m values of pure PLA before and after extrusion treatment were also similar, meaning that no significant degradation of PLA took place.

Table 3. Thermal Properties of PLA and Composites with Different HT-TMPs Before and After Melt Compounding Evaluated from the Second Heating Cycle

Sample type	T_g (°C)	T_m (°C)	Crystallinity (%)
PLA granulates	66 ± 6	159 ± 3	43 ± 2
Ext-PLA	64 ± 1	157.0 ± 0.6	20 ± 2
Ext-TMP 130 2%	63.8 ± 0.6	156.6 ± 0.6	31 ± 3
Ext-TMP 150 2%	61 ± 5	156.6 ± 0.9	29 ± 5
Ext-TMP 170 2%	64.7 ± 0.3	156.7 ± 0.5	34 ± 2
Ext-TMP 130 20%	63.4 ± 0.7	155.8 ± 0.4	35 ± 2
Ext-TMP 150 20%	63.9 ± 0.1	155.5 ± 0.4	34 ± 1
Ext-TMP 170 20%	64.1 ± 0.1	155.3 ± 0.7	34 ± 1

Errors as one standard deviation

The crystallinity values increased after fiber addition, already at very low fiber loading (Table 3): at 2% and 20% fiber content, there was only a small difference in sample crystallinity. It is well known that various solid particles, including natural fibers (Mathew *et al.* 2006; Pilla *et al.* 2009; Pei *et al.* 2010), can act as nucleating sites, thereby increasing the crystallization rate. Both the first and the second heating cycle of DSC indicated that the presence of fibers increased the rate of crystallization. For the second cycle (Table 3), the crystallinities were identical for all TMP types, but for the first cycle the 130 °C TMP crystallized slightly less fast (the first-cycle crystallinities were 13 ± 7% for the pure PLA, 22 ± 5% for the 130 °C TMP, 26 ± 2% for the 150 °C TMP and 30 ± 1% for the 170 °C TMP, when the fiber contents were 20%). The rather high standard deviations indicate greater inhomogeneity in the extruded PLA and the 130 °C TMP composite samples. In general, DSC specimen selection is crucial, and care must be taken to ensure representative results.

The limited crystallization of PLA in injection molding can cause the impairment of mechanical properties (Harris and Lee 2008; Drieskens *et al.* 2009; Sanchez-Garcia and Lagaron 2010), but our data indicate that the introduction of fibers speeds up the crystallization process in the used experimental setup. Transcrystallization, the formation of oriented crystals at the fiber-matrix interface, has been found to dominate in PLA/wood flour composites, where the fiber surface is rough (Mathew *et al.* 2006). Similar crystallization is very likely in these composites as well.

The results for both the crystallinities and the mechanical properties are in line with previously reported values for PLA and pine wood flour (Mathew *et al.* 2006; Pilla *et al.* 2008). Despite the increased crystallinity, the tensile strength remained at its initial level and the impact strength decreased slightly upon the introduction of fibers.

Water Absorption

Water absorption was lowest in pure PLA, as expected (Fig. 7), despite the fact that the specimen densities were practically the same for all sample types (*i.e.*, 1.27 ± 0.01 g/mL). After nearly two weeks of immersion in water, the water absorbance values were 0.7% for PLA, 3.0% for 130 °C TMP, 2.8% for 150 °C TMP, and 2.3% for 170 °C TMP.

These values are very close to the ones obtained by Peltola *et al.* (2014) for PLA/TMP composites with 30 wt.% fiber.

Possibly because of the uneven nature of the composites with 130 °C TMP, their absorption values had higher standard deviations than any other samples. However, it can be concluded that composites with HT-TMPs absorbed less water than composites with the 130 °C TMP, especially in the case of the 170 °C TMP. The reason for this is likely the higher surface coverage by lignin or the loss of hemicelluloses (Sivonen *et al.* 2002; Solala *et al.* 2014), both of which are expected to decrease water absorption on the fiber level. Another thing to consider is that fibers may form a network, through which water can diffuse more efficiently than through the pure polymer (Peltola *et al.* 2014). It is also possible that the presence of fiber agglomerates in the 130 °C TMPs led to the presence of voids, which further increased the water absorption (Peltola *et al.* 2014) but this was not investigated further in the present study due to the fact that the density values were so close to each other. However, the pore size distribution of TMP and HT-TMP could be compared in future studies to further elucidate the reason for the observed difference in water absorbance (see, for example, Maloney and Paulapuro 1999). For future studies, we propose that also the variation in composite and TMP fiber porosities be characterized.

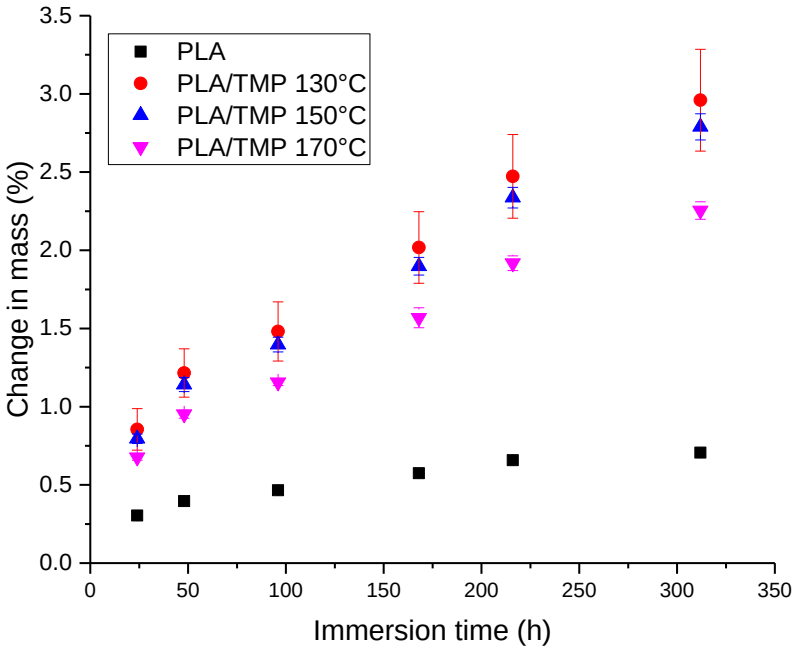

Fig. 7. Water absorption results for pure PLA and composites containing 20 wt.% TMP (three parallel specimens)

Based on the results presented herein, HT-TMP/PLA composites show potential for replacing commodity plastics in an ecological and economical way. Especially in applications where the mechanical properties of pure PLA are sufficient, the inclusion of HT-TMP may enable partial replacement of PLA without compromising the material properties excessively, thus enhancing the competitiveness of PLA in commodity products.

CONCLUSIONS

1. The inherently hydrophobic HT-TMP was evenly dispersed in the PLA matrix, whereas the reference TMP (defibrated at 130 °C) remained partly as visible fiber bundles. It is likely that the low level of fibrillation and the weak fiber-fiber interactions were crucial for achieving efficient mixing.
2. Despite having higher initial aspect ratios, the HT-TMPs were damaged more severely in extrusion and in the end had lower aspect ratios than the 130 °C TMP. Damage to the HT-TMP could be slightly decreased by increasing the mixing rate in the extrusion, but the 130 °C TMP was damaged more at the higher mixing rate.
3. For composites with the highest fiber content (20%), the tensile strengths of the composites remained at approximately the same level as for pure PLA, the Young's moduli increased, but the impact strengths decreased slightly. However, the crystallinity values of the extruded and injection molded specimens increased in the presence of fibers, suggesting that nucleation took place, accelerating the PLA crystallization.

ACKNOWLEDGMENTS

The TEKES-funded project DWoC is acknowledged for financing this work. The authors also gratefully acknowledge Mr. Tommi Lehtinen, Ms. Myrtel Kåll, Ms. Meri Kiviniemi, and Mr. Pasi Seppälä for their assistance in the experiments.

REFERENCES CITED

Ahmed, S., and Jones, F. R. (1990). "A review of particulate reinforcement theories for polymer composites," *J. Mater. Sci.* 25(12), 4933-4942. DOI: 10.1007/BF00580110

Brändström, J., Bardage, S. L., Nilsson, G.D., and Nilsson, T. (2003). "The structural organisation of the S1 cell wall layer of Norway spruce tracheids," *IAWA J.* 24(1), 27-40. DOI: 10.1163/22941932-90000318

Donaldson, L., and Knox, J. P. (2012). "Localization of cell wall polysaccharides in normal and compression wood of radiata pine: Relationships with lignification and microfibril orientation," *Plant Phys.* 158(2), 642-653. DOI: 10.1104/pp.111.184036

Drieskens, M., Peeters, R., Mullens, J., Franco, D., Lemstra, P. J., and Hristova-Bogaerds, D. G. (2009). "Structure versus properties relationship of poly(lactic acid). I. Effect of crystallinity on barrier properties," *J. Polym. Sci. B* 47(22), 2247-2258. DOI: 10.1002/polb.21822

Drumright, R. E., Gruber, P. R., and Henton, D. E. (2000). "Polylactic acid technology," *Adv. Mater.* 12(23), 1841-1846. DOI: 10.1002/1521-4095(200012)12:23<1841::AID-ADMA1841>3.0.CO;2-E

EN ISO 179-1 (2010). "Plastics. Determination of Charpy impact properties. Part 1: Non-instrumented impact test," EU adoption of International Organization for Standardization, Geneva, Switzerland.

EN ISO 527-2 (2012). "Plastics. Determination of tensile properties. Part 2: Test conditions for moulding and extrusion plastics," EU adoption of International Organization for Standardization, Geneva, Switzerland.

EN ISO 62 (2008). "Plastics. Determination of water absorption," EU adoption of International Organization for Standardization, Geneva, Switzerland.

Fu, S. Y., and Lauke, B. (1996). "Effects of fiber length and fiber orientation distributions on the tensile strength of short-fiber-reinforced polymers," *Compos. Sci. Technol.* 56(10), 1179-1190. DOI: 10.1016/S0266-3538(96)00072-3

Fu, S. Y., Lauke, B., Mäder, E., Yue, C. Y., and Hu, X. (2000). "Tensile properties of short-glass-fiber- and short-carbon-fiber-reinforced polypropylene composites," *Compos. Part A* 31(10), 1117-1125. DOI: 10.1016/S1359-835X(00)00068-3

Gamon, G., Evon, P., and Rigal, L. (2013). "Twin-screw extrusion impact on natural fibre morphology and material properties in poly(lactic acid) based biocomposites," *Ind. Crops Prod.* 46, 173-185. DOI: 10.1016/j.indcrop.2013.01.026

Graupner, N. (2008). "Application of lignin as natural adhesion promoter in cotton fibre-reinforced poly(lactic acid) (PLA) composites," *J. Mater. Sci.* 43(15), 5222-5229. DOI: 10.1007/s10853-008-2762-3

Gustafsson, J., Lehto, J. H., Tienvieri, T., Ciovida, L., and Peltonen, J. (2003). "Surface characteristics of thermomechanical pulps; the influence of defibration temperature and refining," *Colloids Surf. A* 225(1-3), 95-104. DOI: 10.1016/S0927-7757(03)00320-0

Harris, A. M., and Lee, E. C. (2008). "Improving mechanical performance of injection molded PLA by controlling crystallinity," *J. Appl. Polym. Sci.* 107(4), 2246-2255. DOI: 10.1002/app.27261

Hietala, M., Samuelsson, E., Niinimäki, J., and Oksman, K. (2011). "The effect of pre-softened wood chips on wood fibre aspect ratio and mechanical properties of wood-polymer composites," *Compos. Part A* 42(12), 2110-2116. DOI: 10.1016/j.compositesa.2011.09.021

Koljonen, K., Österberg, M., Johansson, L. S., and Stenius, P. (2003). "Surface chemistry and morphology of different mechanical pulps determined by ESCA and AFM," *Colloid Surf. A* 228(1-3), 143-158. DOI: 10.1016/S0927-7757(03)00305-4

Le Baillif, M., and Oksman, K. (2009). "The effect of processing on fiber dispersion, fiber length, and thermal degradation of bleached sulfite cellulose fiber polypropylene composites," *J. Thermoplast. Compos.* 22(2), 115-133. DOI: 10.1177/0892705708091608

Li, H., and Sain, M. M. (2003). "High stiffness natural fiber-reinforced hybrid polypropylene composites," *Polym. Plast. Technol.* 42(5), 853-862. DOI: 10.1081/PPT-120024999

Maloney, T. C., and Paulapuro, H. (1999). "The formation of pores in the cell wall," *J. Pulp Pap. Sci.* 25(12), 430-436.

Mathew, A. P., Oksman, K., and Sain, M. (2005). "Mechanical properties of biodegradable composites of poly lactic acid (PLA) and microcrystalline cellulose (MCC)," *J. Appl. Polym. Sci.* 97(5), 2014-2025. DOI: 10.1002/app.21779

Mathew, A. P., Oksman, K., and Sain, M. (2006). "The effect of morphology and chemical characteristics of cellulose reinforcements on the crystallinity of polylactic acid," *J. Appl. Polym. Sci.* 101(1), 300-310. DOI: 10.1002/app.23346

Migneault, S., Koubaa, A., Erchiqui, F., Chaala, A., Englund, K., Krause, C., and Wolcott, M. (2008). "Effect of fiber length on processing and properties of extruded

wood-fiber/HDPE composites," *J. Appl. Polym. Sci.* 110(2), 1085-1092. DOI: 10.1002/app.28720

Migneault, S., Koubaa, A., Erchiqui, F., Chaala, A., Englund, K., and Wolcott, M. P. (2009). "Effects of processing methods and fiber size on the structure and properties of wood-plastic composites," *Compos. Part A* 40(1), 80-85. DOI: 10.1016/j.compositesa.2008.10.004

Nampoothiri, K. M., Nair, N. R., and John, R. P. (2010). "An overview of the recent developments in polylactide (PLA) research," *Bioresour. Technol.* 101(22), 8493-8501. DOI: 10.1016/j.biortech.2010.05.092

Pei, A., Zhou, Q., and Berglund, L. A. (2010). "Functionalized cellulose nanocrystals as biobased nucleation agents in poly(L-lactide) (PLLA) – Crystallization and mechanical property effects," *Compos. Sci. Technol.* 70(5), 815-821. DOI: 10.1016/j.compscitech.2010.01.018

Peltola, H., Pääkkönen, E., and Jetsu, P. (2011). "Effects of of physical pretreatment of wood fibres on fibre morphology and biocomposite properties," *Plast. Rubber Compos.* 40(2), 86-92. DOI: 10.1179/174328911X12988622801016

Peltola, H., Pääkkönen, E., Jetsu, P., and Heinemann, S. (2014). "Wood based PLA and PP composites: Effect of fibre type and matrix," *Compos. Part A* 61, 13-22. DOI: 10.1016/j.compositesa.2014.02.002

Pétrissans, M., Gérardin, P., El bakali, I., and Serraj, M. (2003). "Wettability of heat-treated wood," *Holzforschung* 57(3), 301-307. DOI: 10.1515/HF.2003.045

Pilla, S., Gong, S., O'Neill, E., Rowell, R. M., and Krzysik, A. M. (2008). "Polylactide–pine wood flour composites," *Polym. Eng. Sci.* 48(3), 578-587. DOI: 10.1002/pen.20971

Pilla, S., Gong, S., O'Neill, E., and Rowell, R. M. (2009). "Polylactide–recycled wood fiber composites," *J. Appl. Polym. Sci.* 111(1), 37-47. DOI: 10.1002/app.28860

Roffael, E., Dix, B., and Schneider, T. (2001). "Thermomechanical (TMP) and chemo-thermomechanical pulps (CTMP) for medium density fibreboards (MDF)," *Holzforschung* 55(2), 214-218. DOI: 10.1515/HF.2001.035

Saheb, D. N., and Jog, J. P. (1999). "Natural fiber polymer composites: A review," *Adv. Polym. Technol.* 18(4), 351-363. DOI: 10.1002/(SICI)1098-2329(199924)18:4<351::AID-ADV6>3.0.CO;2-X

Salmén, L. (1982) "Temperature and water induced softening behaviour of wood fiber based materials," Doctoral Thesis, The Royal Institute of Technology, Sweden

Sanchez-Garcia, M. D., and Lagaron, J. M. (2010). "On the use of plant cellulose nanowhiskers to enhance the barrier properties of polylactic acid," *Cellulose* 17(5), 987-1004. DOI: 10.1007/s10570-010-9430-x

Sivonen, H., Maunu, S. L., Sundholm, F., Jämsä, S., and Viitaniemi, P. (2002). "Magnetic resonance studies of thermally modified wood," *Holzforschung* 56(6), 648-654. DOI: 10.1515/HF.2002.098

Solala, I., Antikainen, T., Reza, M., Johansson, L. S., Hughes, M., and Vuorinen, T. (2014). "Spruce fiber properties after high-temperature thermomechanical pulping (HT-TMP)," *Holzforschung* 68(2), 195-201. DOI: 10.1515/hf-2013-0083

TAPPI T271 om-98 (2007). "Fiber length of pulp and paper by automated optical analyzer using polarized light," TAPPI Press, Atlanta, GA.

TAPPI T261 pm-80 (1989). "Fines fraction by weight of paper stock by wet screening – Britt Jar," TAPPI Press, Atlanta, GA.

Valenzuela, J., von Leyser, E., Pizzi, A., Westermeyer, C., and Gorrini, B. (2012). "Industrial production of pine tannin-bonded particleboard and MDF," *Eur. J. Wood Prod.* 70(5), 735-740. DOI: 10.1007/s00107-012-0610-2

Wambua, P., Ivens, J., and Verpoest, I. (2003). "Natural fibres: Can they replace glass in fibre reinforced plastics?" *Compos. Sci. Technol.* 63(9), 1259-1264. DOI: 10.1016/S0266-3538(03)00096-4

Widsten, P., and Kandelbauer, A. (2008). "Laccase applications in the forest products industry: A review," *Enzyme Microb. Tech.* 42(4), 293-307. DOI: 10.1016/j.enzmictec.2007.12.003

Widsten, P., Laine, J. E., Qvintus-Leino, P., and Tuominen, S. (2001). "Effect of high-temperature fiberization on the chemical structure of softwood," *J. Wood Chem. Technol.* 21(3), 227-245. DOI: 10.1081/WCT-100105374

Widsten, P., Tuominen, S., Qvintus-Leino, P., and Laine, J. E. (2004). "The influence of high defibration temperature on the properties of medium-density fiberboard (MDF) made from laccase-treated softwood fibers," *Wood Sci. Technol.* 38(7), 521-528. DOI: 10.1007/s00226-003-0206-4

Wu, J. Q., Wen, J. L., and Sun, R. C. (2015). "Integrated hot-compressed water and laccase-mediator treatments of Eucalyptus grandis fibers: Structural changes of fiber and lignin," *J. Agric. Food Chem.* 63(6), 1763-1772. DOI: 10.1021/jf506042s

Xing, C., Riedl, B., Cloutier, A., and Shaler, S. M. (2005). "Characterization of urea–formaldehyde resin penetration into medium density fiberboard fibers," *Wood Sci. Technol.* 39(5), 374-384. DOI: 10.1007/s00226-005-0294-4

Yin, Y., Berglund, L., and Salmén, L. (2011). "Effect of steam treatment on the properties of wood cell walls," *Biomacromolecules* 12(1), 194-202. DOI: 10.1021/bm101144m

Article submitted: August 14, 2015; Peer review completed: November 16, 2015; Revised version received and accepted: November 24, 2015; Published: December 9, 2015.
DOI: 10.15376/biores.11.1.1125-1140